Middle East Journal of Science

https://dergipark.org.tr/mejs **MEJS**

e-ISSN:2618-6136

Research Article

PREPARATION AND CHARACTERIZATION OF ACTIVATED CARBON FROM ACORN CUPS VIA HCl-$FeCl_2$ CO-ACTIVATION FOR HYDROGEN GENERATION THROUGH $NABH_4$ SOLVOLYSIS

Uğur IŞIK* [1]

[1] Artvin Coruh University, Medicinal-Aromatic Plants Specialization Coordinatorship, Artvin, 08100, Türkiye
*Corresponding author ugurisik@artvin.edu.tr

Abstract: *This current study reports the synthesis, characterization, and optimization of a novel catalyst (Ac-HCl-Fe) derived from Acorn cups biomass waste for hydrogen production via sodium borohydride ($NaBH_4$) solvolysis. The catalyst characterization was conducted using FTIR, SEM, and SEM-EDX techniques. Catalytic performance tests showed the efficiency of Ac-HCl-Fe in hydrogen generation, with parameters including catalyst loading, $NaBH_4$ quantity, and reaction temperature significantly influencing the kinetics. Remarkably, the $NaBH_4$ methanolysis reaction catalyzed by Ac-HCl-Fe was completed in 4.0 minutes, while the $NaBH_4$ solvolysis in a binary propylene glycol/methanol (1:1, v/v) solvent system reached completion within just 0.9 minutes, producing a similar volume of hydrogen (~670 mL). The HGR was determined to be 68,300 $mL\ min^{-1}g_{cat}^{-1}$ for the $NaBH_4$ solvolysis reaction conducted in a binary propylene glycol/methanol (1:1, v/v) solvent system at 30 °C. In addition, the effective activation energy was calculated to be 32.36 kJ/mol, that is relatively low compared to other activated carbon-based catalysts reported for similar applications. Overall, the results show that Ac-HCl-Fe is a promising, efficient, and sustainable catalyst for hydrogen generation by solvolysis of $NaBH_4$, especially in binary solvent systems.*

Keywords: *Hydrogen generation, Sodium borohydride, Solvolysis, Propylene glycol, Binary solvent system.*

Received: October 17, 2025 *Accepted: December 16, 2025*

1. Introduction

Energy underpins virtually every dimension of contemporary society, enabling activities that range from household functions and mobility to industrial manufacturing and digital infrastructures [1, 2]. Despite sustained advances in renewable technologies and efficiency policy, the primary energy mix of major economies remains dominated by fossil resources, principally petroleum, natural gas, and coal, which together still supply in excess of four-fifths of global energy demand [2-4]. This path dependence derives from the historically favourable cost, energy density, and supply-chain maturity of fossil fuels; however, it simultaneously exposes the global economy to sustainability and security pressures as finite reserves are consumed at scale [4-6]. Reserve-to-production assessments consistently indicate bounded temporal horizons—on the order of ~60 years for natural gas, ~40 years for petroleum, and ~156 years for coal under prevailing conditions—underscoring the structural risks of continued overreliance on depleting stocks [7]. Accordingly, accelerating the deployment of renewable energy systems is widely viewed as indispensable for a credible transition toward net-zero emissions, with the added benefit of long-term economic co-gains relative to the status quo [8].

Within this transition, hydrogen has emerged as a versatile energy vector and feedstock capable of decarbonizing multiple hard-to-abate sectors (e.g., chemicals, refining, steel, and dispatchable power), while producing zero carbon emissions at the point of use [9]. Its appeal rests on high specific energy on a mass basis and the possibility of flexible production pathways (electrolysis, reforming with carbon capture and biomass routes), which can ultimately sever the strong coupling between energy services and fossil carbon. Yet the promise of a hydrogen economy is contingent on solving materials and systems challenges, foremost among them safe, dense, and energy-efficient storage.

Hydrogen storage remains technically demanding because H_2, the smallest neutral molecule, is highly diffusive and buoyant, which complicates containment and logistics. Conventional mechanical options, compressed gas cylinders and cryogenic liquid storage have been used for decades, but they incur substantial energy penalties and capital costs for compression/liquefaction, boil-off management, and robust containment [6]. These limitations have motivated intensive research into alternative approaches, including cryo-compression, chemical hydrogen carriers (hydrides and liquid organic hydrogen carriers), and physisorption on high-surface-area materials such as activated carbons and related porous solids [6,10]. Among chemical hydrides, compounds such as lithium borohydride, lithium hydride, sodium borohydride, magnesium hydride, and ammonia borane are notable for their relatively high gravimetric hydrogen contents and ambient-temperature stability, making them attractive candidates for controllable on-demand H_2 release [11, 12].

Sodium borohydride ($NaBH_4$) is particularly compelling within this class because it combines high theoretical hydrogen capacity with several practical advantages: it is non-volatile and non-flammable in the solid state, can be handled comparatively safely, and is capable of generating hydrogen without the elevated temperatures often required by metal hydrides [13]. In alcoholysis routes, $NaBH_4$ reacts with alcohols to liberate hydrogen while forming borate esters. For methanol (CH_3OH) and propylene glycol ($CH_3CH(OH)CH_2OH$), the overall stoichiometries can be represented as Eqs. (1) and (2).

$$NaBH_4 + 4CH_3OH \rightarrow 4H_2 + NaB(OCH_3)_4 \quad (1)$$

$$NaBH_4 + 2CH_3CH(OH)CH_2OH \rightarrow 4H_2 + NaB(C_3H_6O_2)_2 \quad (2)$$

While $NaBH_4$ hydrolysis is a well-studied pathway for hydrogen generation, it is constrained at sub-zero temperatures by water freezing and the concomitant mass-transfer limitations in aqueous media [14]. Substituting alcohol for water mitigates these issues. Methanol is especially attractive because it enables rapid reaction kinetics even below 0 °C, and the borate ester by-product, $NaB(OCH_3)_4$, is highly soluble in methanol. High solubility reduces operational challenges like line clogging and catalyst fouling, which promotes smoother continuous operation [15]. Propylene glycol likewise supports $NaBH_4$ alcoholysis and offers additional handling advantages: it is substantially less toxic than methanol and exhibits a density comparable to water (≈1.036 vs. 1.0 g cm^{-3}), which can simplify process integration and materials compatibility [16]. Despite these benefits, further improvements in activity, selectivity, and cost are required to translate $NaBH_4$ alcoholysis into robust, scalable hydrogen-on-demand systems; in particular, the development of efficient and economical catalysts remains a critical lever [17, 18].

Both homogeneous and heterogeneous catalysts have been explored to accelerate $NaBH_4$ alcoholysis, with heterogeneous systems favoured for their ease of separation, recyclability, and process stability [19-21]. By lowering activation barriers and furnishing active sites for hydride transfer and B–H bond activation, these catalysts substantially increase the hydrogen generation rate (HGR) under controlled conditions [22]. Architecturally, catalysts can be classified as unsupported or supported; common carbonaceous supports include activated carbon[23], graphene oxide[24], and carbon nanotubes[25], each providing high surface area and tunable surface chemistry for dispersing catalytically active phases. Although precious metal-containing catalysts (e.g., Pd, Rh, Ru, Pt) often

deliver outstanding intrinsic activity, their high cost and limited natural abundance constrain large-scale deployment [26]. Consequently, there is strong impetus to engineer catalysts based on earth-abundant, low-cost transition metals (Cu, Co, Ni, Fe), which have demonstrated promising activity profiles when appropriately structured and supported [27-29].

In this context, the use of bio-waste as a catalyst carrier offers a cost-effective and environmentally friendly alternative. The properties of carbon materials derived from natural precursors strongly depend on their intrinsic structure, composition, and the applied preparation method [30]. In particular, porous carbon materials are regarded as promising candidates for various applications, especially in electrochemical energy storage and catalysis, due to their unique characteristics, including high porosity, low weight, physicochemical stability, and excellent electrical conductivity [31]. These materials offer high specific surface areas (typically 500-3000 m^2/g), tunable pore structures, chemical inertness, and the ability to support active metal species while participating directly in catalytic processes. Among various bio-derived sources, acorn cups represent an abundant lignocellulosic waste rich in carbon precursors and tannins, making them suitable for conversion into porous carbon structures. In this study, an activated carbon material was successfully synthesized from bio-waste derived from acorn cups (Ac), through chemical activation with HCl and $FeCl_2$ followed by straightforward carbonization process under an inert gas atmosphere. The resulting biochar catalyst, referred to as **Ac-HCl-Fe**, is designed to be environmentally friendly, low-cost, and easily obtainable. This study further investigates the influence of binary solvent systems as alternatives to conventional single-component solvents in $NaBH_4$ methanolysis. In the first stage, methanol was used as the primary solvent, and various mixtures with glycol were optimized to identify the most effective solvent composition. In the second stage, the catalytic performance of the activated carbon-based material was evaluated under the optimized propylene glycol/methanol reaction conditions.

2. Experimental Section

2.1. Materials and Reagents

Analytical-grade reagents and chemicals were employed throughout the study and were utilized immediately upon receipt. Chemicals used for solvolysis, and catalyst preparation included iron(II) chloride ($FeCl_2$), $NaBH_4$ (98%), propylene glycol (99.5%), hydrochloric acid (HCl, 36.5–38%), and potassium hydroxide (KOH, anhydrous, ≥99.95%), all purchased from Sigma-Aldrich or Merck. The methanol employed in the catalytic experiments (≥99.9% (GC), suitable for LC/MS; Supelco) was utilized directly without any additional purification. The Milli-Q direct water purification system was used to obtain distilled water. Prior to the experiments, all glassware was carefully washed with acetone, rinsed with distilled water, and dried at 80 °C.

2.2. Methods

2.2.1 Ac-HCl-Fe Catalyst Preparation

In this study, Ac-HCl-Fe, used as a catalyst, was prepared by making minor modifications to the method reported by Kalkan [32]. The Ac-HCl-Fe catalyst was prepared by adding 30% $FeCl_2$ by weight and 25 mL of 30% HCl solution to 3 g of acorn cups (Ac) and the mixture was stirred at 750 rpm for 1 hour at room temperature. The sample was then dried at a temperature of 85 °C for 24 hours and then carbonized at a temperature of 400 °C for 60 minutes. To enable the use of the activated carbons as catalysts, they were first ground to a particle size of 500 microns and then washed with 0.5 M HCl and KOH solutions. Following the washing procedure, the samples were subjected to rinsing with deionized water until the pH attained a neutral equilibrium, after which they were subsequently

desiccated. The obtained activated carbons were stored under appropriate conditions for subsequent experiments.

The catalytic performance of the synthesized samples was assessed for hydrogen generation from $NaBH_4$, with particular emphasis on the hydrogen generation rate (HGR) and activation energy. The measurement system comprised three components: a temperature control heater, a reaction vessel, and a gas collector. The volume of H_2 gas produced was determined by water displacement and plotted versus time. Subsequently, the selected high-performance catalyst was characterized using SEM, SEM-EDX, and FTIR analyses.

2.2.2 Characterization of the Ac-HCl-Fe Catalyst

FTIR with a Shimadzu IR Prestige-21 spectrometer was used to determine the functional groups. The morphological properties of the acorn cups (Ac) and Ac-HCl-Fe catalyst were investigated by scanning electron microscopy (SEM, Carl Zeiss EVO LS10). The elemental distribution on the catalyst was analyzed by using energy-dispersive X-ray spectroscopy (EDS, Bruker XFlash 6160), and the average data from three different regions for each sample were reported.

2.2.3 Hydrogen Production Measurements

Experiments on the $NaBH_4$ dehydrogenation in methanol (M) or propylene glycol/methanol (PG/M) using the Ac-HCl-Fe catalyst were conducted via the water displacement method. In each experiment, predetermined amounts of Ac-HCl-Fe catalyst (0.0125–0.05 g) and $NaBH_4$ (0.1–0.75 g) were introduced into a 50 mL reaction vessel maintained at 20–50 °C. In methanol reactions, 10 mL of M was employed, whereas the optimized PG/M system comprised 5 mL each of methanol and propylene glycol, added via syringe. The hydrogen generated volume during solvolysis was measured based on the volume of water displaced by reaction. All experiments were conducted at Artvin Coruh University (altitude: 345 m), where atmospheric pressure was considered 0.98 atm for theoretical hydrogen volume calculations (~670 mL). The hydrogen generation rate (HGR) was determined from the slope of the hydrogen volume versus time plots. As presented in equation (3), HGR is defined as the volume of hydrogen produced per unit time per unit catalyst and is calculated by dividing the measured hydrogen volume by the amount of catalyst used and the reaction time.

$$\text{HGR} = \text{Measured Hydrogen Volume} / (\text{Used Catalyst Amount X Elapsed Time}) \quad (3)$$

Repeatability tests for the Ac-HCl-Fe catalyst were performed at 30 °C using $NaBH_4$ (0.25 g), catalyst (0.025 g), and PG/M mixture (1:1, v/v, 10 mL). Following each run, the catalyst was recovered via centrifugation, oven-dried, and reused. These tests were conducted sequentially over five cycles, with 0.25 g $NaBH_4$ added at the end of each cycle to initiate the subsequent reaction.

3. Results And Discussion

3.1. Prepared Ac-HCl-Fe Catalyst for Characterization

3.1.1 SEM and EDS Analyses

The SEM study was performed on raw acorn cups (Ac) and Ac-HCl-Fe to examine the alterations in Ac's surface morphology prior to and following HCl-$FeCl_2$ co-activation, as well as of the catalyst (Ac-HCl-Fe) synthesized through chemical activation. As seen in Fig. 1, Ac and Ac-HCl-Fe exhibit significant differences in terms of microscopic morphology and porous structure. The SEM images reveal that raw acorn cups exhibit a relatively smooth and larger-particle structure, whereas Ac-HCl-Fe displays a rough texture with numerous small pores and particles, indicating a higher specific surface area. The primary reasons for this may include simultaneous processes during activation in

which most of the volatile organics are released [33], or co-activation of HCl-$FeCl_2$ may have had a significant effect in improving the catalyst pore structure. The EDX spectrum of the Ac-HCl-Fe sample shows a high content of carbon (53.34%), oxygen (16.48%), magnesium (0.16%), calcium (0.37%), iron (23.36%) and chloride (6.29%). These results indicate that acorn cups have a high carbon content, supporting their potential as a precursor for activated carbon, whereas the presence of iron and chloride is attributed to HCl-$FeCl_2$ used during co-activation.

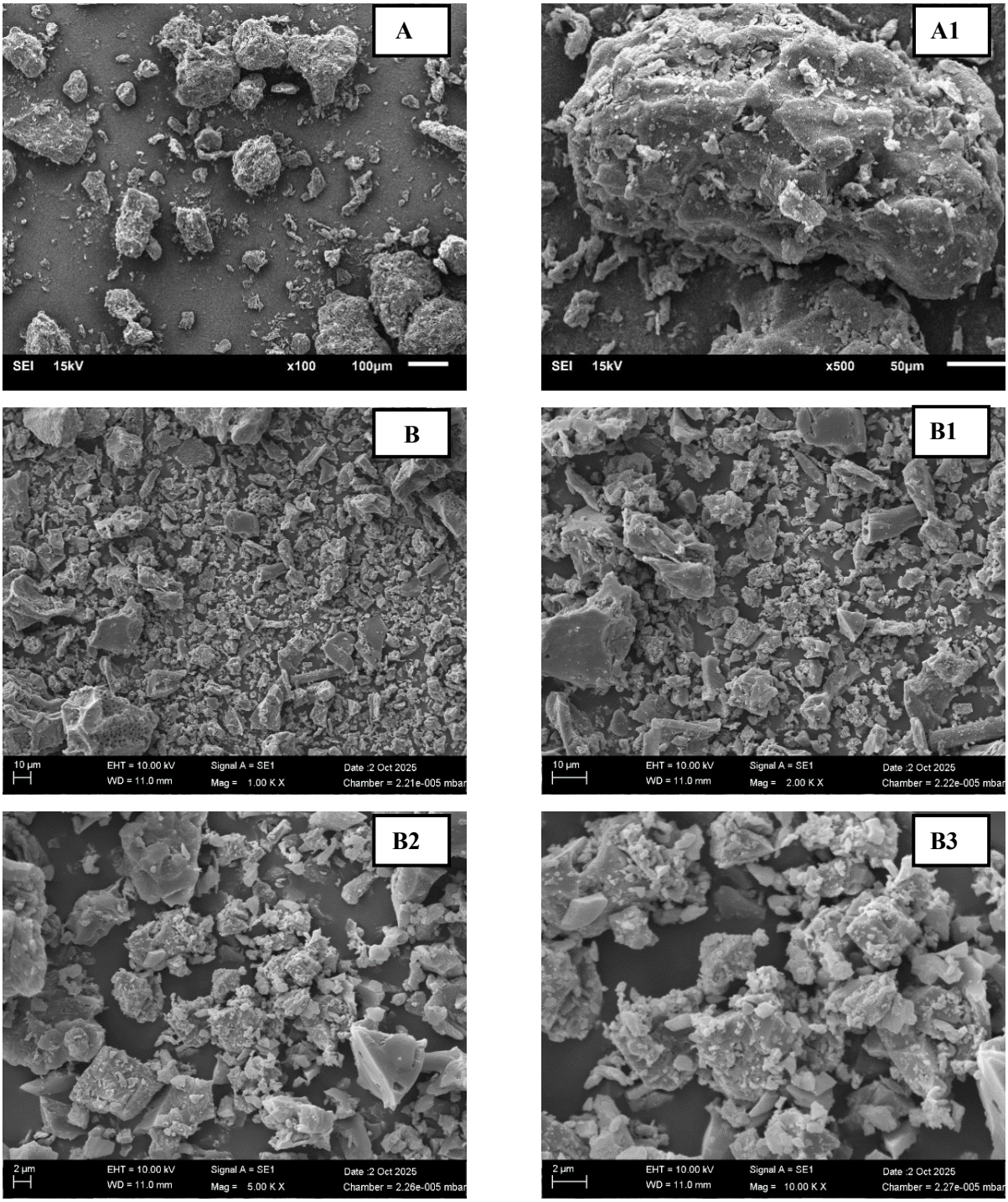

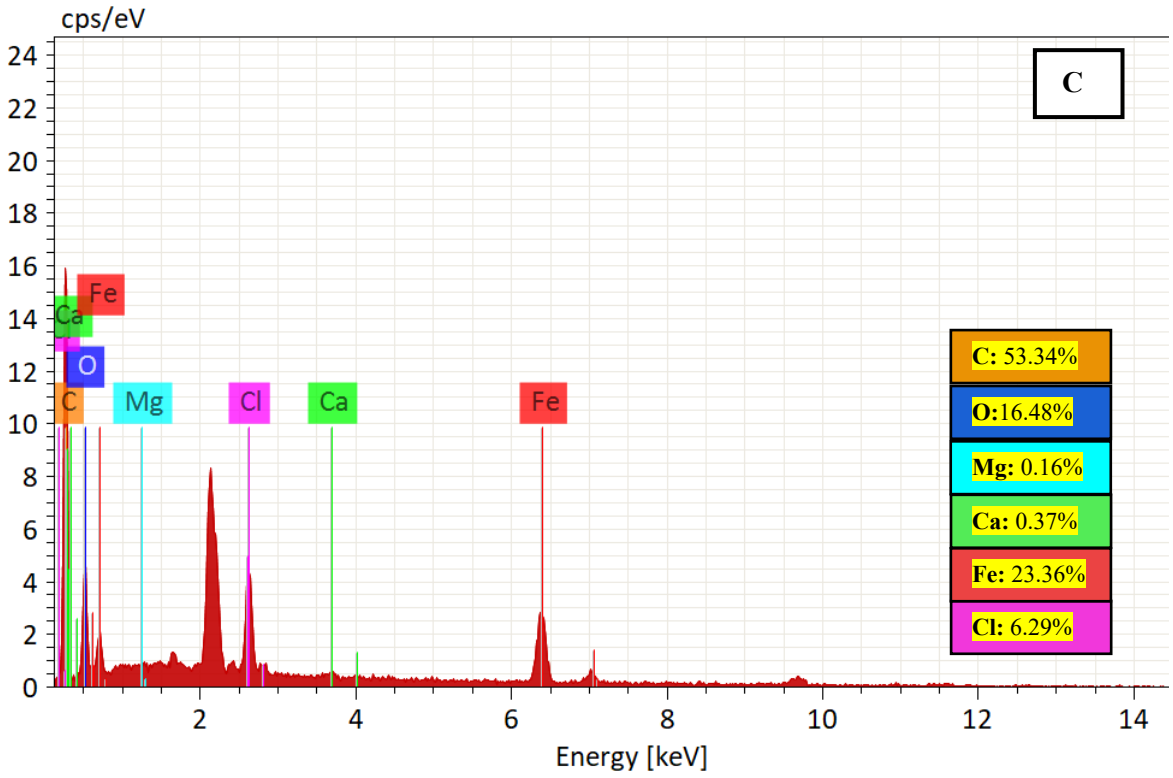

Fig. 1. Microstructural SEM images of acorn cups (Ac) (A–A1); **Ac-HCl-Fe** catalyst (B–B4); and EDS spectra of the **Ac-HCl-Fe** catalyst (C).

3.1.2 FTIR Analysis

FTIR analysis was performed to characterize the raw acorn cups (Ac) and Ac-HCl-Fe, providing detailed information about the molecular structure and chemical composition of the samples. The Ac-HCl-Fe catalyst FTIR spectra, prepared via HCl-$FeCl_2$ co-activation and pyrolyzed at 400 °C for 60 minutes from Ac, are shown in Fig. 2. Compared to Ac-HCl-Fe, the Ac sample contains a greater number of surface functional groups. In particular, the broad band observed between 3200 and 3600 cm^{-1} corresponds to O–H and/or N–H stretching vibrations, indicating the presence of phenolic compounds and alcohols. The C–H stretching vibrations observed at 2850–2920 cm^{-1} [34, 35] and the C–H bending vibrations at 1350–1440 cm^{-1} are attributed to aliphatic hydrocarbon chains (alkanes) [36, 37]. The bands at 1611 cm^{-1} correspond to C=C stretching vibrations, suggesting the presence of alkene groups [38]. The C=O stretching vibrational bands around 1735 cm^{-1} correspond to the presence of functional groups such as ketones, carboxylic acids, aldehydes, or esters [39]. The band at 1020 cm^{-1} is primarily assigned to the C–OH and C–O–C stretching vibrations of oxygen-containing functional groups in the cellulose structure [40, 41]. These data indicate that raw acorn cups (Ac) contains both aromatic and aliphatic hydrocarbon structures. In the Ac-HCl-Fe catalyst, the -OH absorption band at 3335 cm^{-1}, and the characteristic stretching vibrations of $-CH_2$ at 2865 cm^{-1} and 2948 cm^{-1}, completely disappeared in Ac. Owing to its Lewis acid character, $FeCl_2$ can catalytically promote Friedel–Crafts-type reactions between aromatic hydrocarbons, ketones, aldehydes, and nucleophilic functional groups. These observations clearly demonstrate that the cellulose or hemicellulose chains were extensively degraded at 400 °C, implying that substantial pyrolysis had occurred at this stage. Moreover, the Ac-HCl-Fe catalyst was found to contain a significant number of oxygen-containing functional groups. This suggests that even after the chemical activation with HCl-$FeCl_2$, the acidic oxygen-containing groups

on the surface of the Ac-derived catalyst remain present, and that these surface properties are highly favourable for H_2 generation from $NaBH_4$.

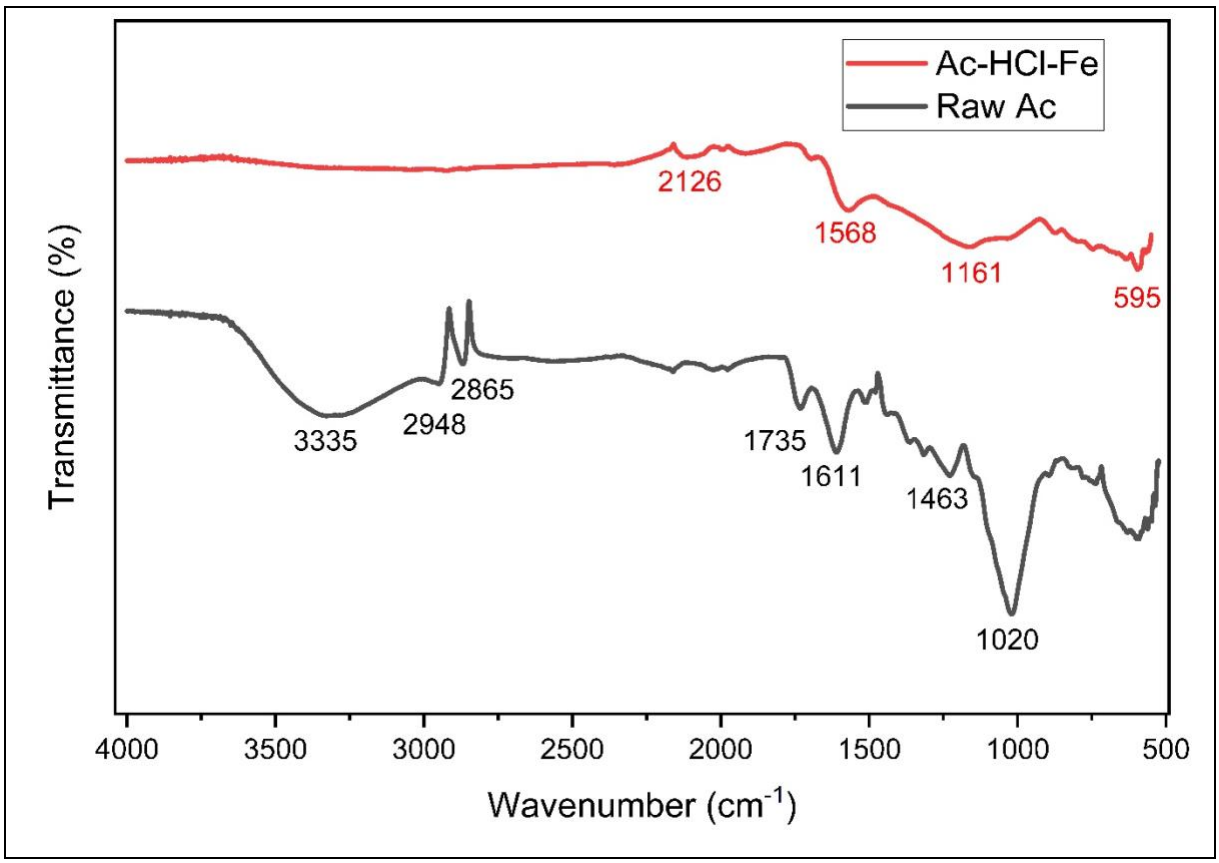

Fig. 2. FT-IR spectra of acorn cups (Ac) and the **Ac-HCl-Fe** catalyst.

3.2. Prepared Ac-HCl-Fe Catalyst for Characterization

$NaBH_4$ methanolysis experiments were conducted using a catalyst prepared by functionalizing acorn cups (Ac) with HCl-$FeCl_2$ co-activation. The experimental parameters were kept constant; the catalyst amount was set at 0.1 g, $NaBH_4$ amount at 0.25 g, the reaction temperature at 30 °C, carbonization temperature and time at 400 °C to 60 min. During the $NaBH_4$ alcoholysis or hydrolysis process, catalysts typically exhibit a gradual decrease in the hydrogen generation rate (HGR), making it challenging to determine the HGR accurately. To simplify the assessment of catalytic activity, the average HGR per gram of catalyst was calculated using the slope of the hydrogen generation curves for each reaction [42, 43]. The hydrogen gas volume and HGR formed as a result of the methanolysis reaction were evaluated in relation to time and the data obtained are presented in Fig. 3a. As shown in Fig. 3a, the reaction reached completion in 8.5 min/1725 $mLmin^{-1}g_{cat}^{-1}$ for raw Ac, whereas HCl-$FeCl_2$ co-activation Ac-HCl-Fe catalyst achieved 100% conversion within 4 min/3861 $mLmin^{-1}g_{cat}^{-1}$. This result indicates that HCl-$FeCl_2$ treatment enhances the catalyst performance, leading to higher hydrogen generation rates (HGRs). Comparable results have been documented by Bekirogulları [44], who synthesized a catalyst from defatted spent coffee grounds using $ZnCl_2$ as an activating agent and achieved the highest HGR of 3205 $mLmin^{-1}g_{cat}^{-1}$ within 4.5 min when 40 wt.% $ZnCl_2$ was used (carbonization temperature and time at 400 °C to 45 min). In another study, Karakaş [21] treated orange peels with HCl, H_2SO_4, and CH_3COOH acids, and reported the HGRs and durations for the resulting catalysts as 2682 $mLmin^{-1}g_{cat}^{-1}$ (5.8 min), 2786 $mLmin^{-1}g_{cat}^{-1}$ (5.75 min), and 2910 $mLmin^{-1}g_{cat}^{-1}$ (5.25

min), respectively. These studies collectively emphasize the critical role of optimized activator conditions in enhancing catalytic performance for hydrogen generation.

Fig. 3b demonstrates the hydrogen volumes and rates at 30 °C when using a catalyst of 25 mg and 0.25 g $NaBH_4$ with different ratios of methanol to propylene glycol (from 10:0 to 0:10). It was noted that the reaction completion time varied depending on the solvent ratio. The reaction times for different methanol/propylene glycol mixtures (10:0, 9:1, 7:3, 5:5, 3:7, 1:9, 0:10) were measured as 6.75, 2.17, 0.92, 0.92, 1.67, 2.50 and 4.83 minutes, respectively. When the results were compared, the highest HGR value (68300 $mLmin^{-1}g_{cat}^{-1}$) was achieved with the 5:5 propylene glycol/methanol mixture, so the 5:5 (1:1) propylene glycol/methanol ratio was selected. This optimal 1:1 ratio is likely due to the balance between solvent polarity and viscosity. Based on these data, the 5:5 propylene glycol/methanol mixture was found to be the most suitable solvent medium for hydrogen production. The propylene glycol and methanol pKa values at 25 °C are 14.9 and 15.2, respectively, and propylene glycol has a more acidic nature. This result is thought to be related to the acidic and viscosity characteristics of propylene glycol and methanol. Since the $NaBH_4$ methanolysis reaction occurs more efficiently in acidic medium, increasing the solvent acidic character may positively affect the reaction kinetics. Therefore, higher hydrogen generation can be anticipated in a medium containing only propylene glycol. In contrast, the viscosities of propylene glycol and methanol at 20 °C are 56 cP and 0.59 cP, respectively. In this context, methanol, which contains the hydroxyl functional group, has a remarkably lower viscosity compared to propylene glycol, which may enable the reaction kinetics to be accelerated. Thus, the propylene glycol/methanol mixture provides a solvent medium that optimizes the hydrogen production from $NaBH_4$ due to the synergistic effect of the methanol low viscosity and the propylene glycol highly acidic character [45]. In addition, Fig. 3b presents the hydrogen production rates in pure methanol and in the propylene glycol/methanol (1:1) mixture. The HGR values obtained in these environments were determined as 8486 and 68300 $mLmin^{-1}g_{cat}^{-1}$, respectively. The reaction completion times were recorded as 6.75 min in methanol medium and only 0.92 min in propylene glycol/methanol (1:1) mixture. The results show that the HGR obtained in the propylene glycol/methanol medium is approximately ten times higher than that in the methanol medium, indicating a significant improvement in catalytic performance. For the remainder of this study, the propylene glycol/methanol mixture in 1:1 ratio, identified as the optimal solvent combination, will be referred to as 'propylene glycol/methanol (PG/M)'.

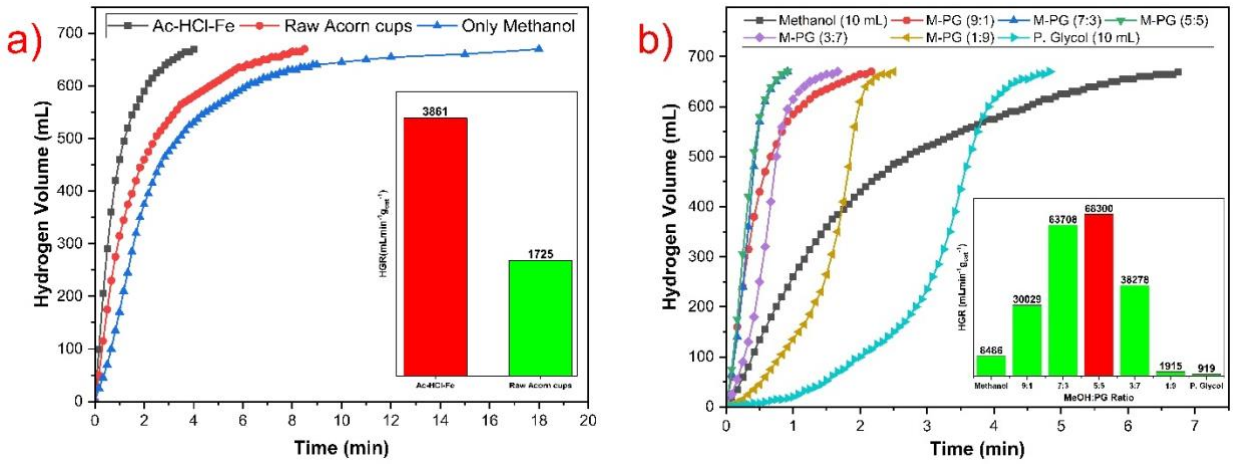

Fig. 3. Effects of (a) AC-HCl-Fe and raw acorn cups catalysts, as well as the self-methanolysis reaction, and (b) solvent type on the hydrogen volume and HGR. [Reaction conditions: (a) 0.1 g catalyst, 0.25 g $NaBH_4$, 10 mL methanol, 30 °C; (b) 0.025 g catalyst, 0.25 g $NaBH_4$, 10 mL solvent, 30 °C].

In the second section, the catalyst synthesized under optimized conditions (30 wt% $FeCl_2$ and 25 mL of 30% HCl solution per 3 g of acorn cups (Ac), carbonized at 400 °C for 60 minutes) was used in performance evaluation experiments, conducted in the optimal 1:1 propylene glycol/methanol mixture. The catalyst loading influence on the HGR was investigated as the first parameter, with the results displayed in Fig. 4a. It was observed that increasing the amount of Ac-HCl-Fe reduced the reaction time for $NaBH_4$ solvolysis. The corresponding reaction times and HGR values for catalyst loadings of 12.5, 25, 37.5 and 50 mg were determined to be 0.92 min/76240 $mLmin^{-1}g_{cat}^{-1}$, 0.92 min/67820 $mLmin^{-1}g_{cat}^{-1}$, 0.83 min/47413 $mLmin^{-1}g_{cat}^{-1}$ and 0.83 min/39460 $mLmin^{-1}g_{cat}^{-1}$, respectively. It is evident that the reaction reaches equilibrium faster as the catalyst amount increases from 12.5 to 50 mg, indicating that a higher catalyst loading substantially shortens the reaction time for $NaBH_4$ methanolysis under identical conditions.

Fig. 4b illustrates the varying $NaBH_4$ amounts effect on the solvolysis reaction catalyzed by AC-HCl-Fe. The experiments were conducted at 30 °C using 25 mg of AC-HCl-Fe catalyst and 10 mL of a propylene glycol/methanol 1:1 mixture, with $NaBH_4$ amounts ranging from 0.1 g to 0.75 g. The corresponding HGR and reaction times were determined as 21209 $mLmin^{-1}g_{cat}^{-1}$/0,92 min (0.1 g), 67820 $mLmin^{-1}g_{cat}^{-1}$/1 min (0.25 g), 79540 $mLmin^{-1}g_{cat}^{-1}$/1.92 min (0.375 g) and 101960 $mLmin^{-1}g_{cat}^{-1}$/2.33 min (0.75 g). Increasing the $NaBH_4$ amount from 0.1 g to 0.25 g resulted in a 3-fold increase in HGR. These experimental results clearly show that the HGR is strongly affected by the amount of $NaBH_4$ used, as illustrated in Fig. 4b. A similar observation has also been reported by Khan et al. [46].

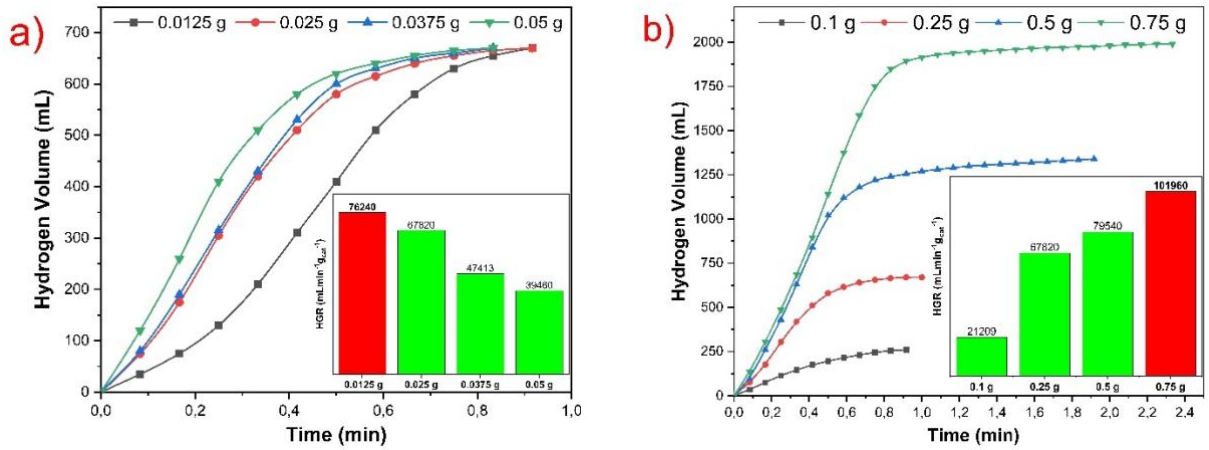

Fig. 4. Effect of (a) catalyst loading and (b) $NaBH_4$ amount on the total hydrogen volume and HGR. [**Reaction condition:** 12.5-50 mg **Ac-HCl-Fe** catalyst, 10 mL propylene glycol/methanol (1:1, v/v) mixture, 0.1-0.75 g $NaBH_4$, 30 °C].

Fig. 5a illustrates the temperature effect on hydrogen release from $NaBH_4$ (0.25 g) in a 10 mL propylene glycol/methanol mixture (1:1, v/v) using 25 mg of the Ac-HCl-Fe catalyst. The experiments were conducted at four temperatures (50, 40,30, and 20 °C) to analyse the temperature effect on reaction performance, yielding HGR values of 143,484; 88,208; 67,820; and 46,660 $mLmin^{-1}g_{cat}^{-1}$, respectively. These results demonstrate that temperature has a significant influence on the H_2 release rate. As observed, HGR at 50 °C was approximately four times higher than that at 20 °C, confirming the expected increase in HGR with rising temperature. The literature reports that the correlation between HGR and temperature is exponential. For comparison, a Chit-Mont-H catalyst was tested in a propylene glycol/ methanol mixture at 50, 40, 30, and 20 °C, yielding hydrogen production rates of 45,264; 31,000; 23,536; and 12,249 $mLmin^{-1}g_{cat}^{-1}$, respectively [45]. These results suggest that Ac-HCl-Fe exhibits

catalytic performance comparable to, or even surpassing, that of similar catalysts reported in the literature. Furthermore, the activation energy (Ea) for hydrogen generation from $NaBH_4$ in propylene glycol/methanol using the Ac-HCl-Fe catalyst was calculated using the Arrhenius equation (Eq. (4)).

$$\ln(k) = \ln(A) - Ea/RT \quad (4)$$

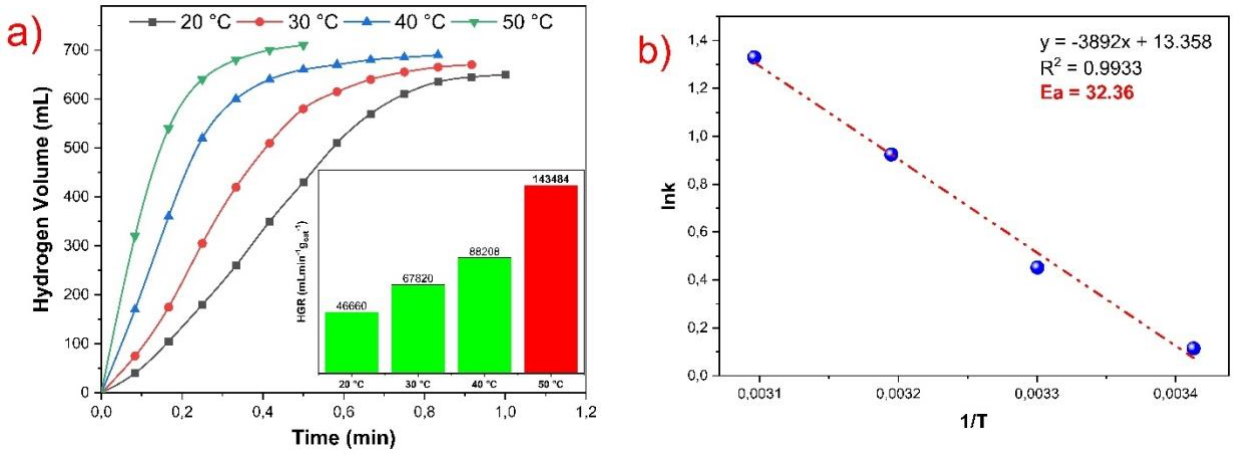

Fig. 5. (a) Influence of reaction temperature on hydrogen production from $NaBH_4$ in a propylene glycol/methanol (1:1, v/v) solvent system using the **Ac-HCl-Fe** catalyst; (b) corresponding Arrhenius plot. [**Reaction condition:** 25 mg catalyst, 10 mL propylene glycol/methanol (1:1, v/v) mixture, 0.25 g $NaBH_4$].

The activation energy for the $NaBH_4$ solvolysis in propylene glycol/methanol catalyzed with Ac-HCl-Fe, was determined to be 32.96 kJ/mol (Fig. 7b), which agrees with the literature values and surpasses those reported in most studies. Furthermore, Table 1 summarizes the Ac-HCl-Fe catalytic efficiency in hydrogen generation compared to catalysts reported in previous studies. In comparison, $NaBH_4$ solvolysis catalysed by **Ac-HCl-Fe** demonstrated excellent kinetic performance, with a significantly higher HGR (67820 $mLmin^{-1}g_{cat}^{-1}$) than most metal catalysts. Moreover, as shown in Table 1, the Ea or HGR of Ac-HCl-Fe is comparable to or better than other catalysts reported in the literature, such as ZnPc (28.47 kJ/mol), GW-HCl-Ni-Cat (18.68 kJ/mol), MPÇ-HCl-Ni-kat (20.43 kJ/mol), Chit/Mont/H (27.53 kJ/mol for propylene glycol/methanol), SSMS-$ZnCl_2$-CoB (31.13 kJ/mol), P-doped g-C_3N_4 (30.30 kJ/mol), N,P-doped Chit@kaolin (17.20 kJ/mol), Co@AC (31.19 kJ/mol, 8593 $mLmin^{-1}g_{cat}^{-1}$), Co@CHE (55.6 kJ/mol, 32036 $mLmin^{-1}g_{cat}^{-1}$), Co@VHE (55.0 kJ/mol, 36624 $mLmin^{-1}g_{cat}^{-1}$), Ru@CQDs (38.19 kJ/mol, 167588 $mLmin^{-1}g_{cat}^{-1}$) and DS-HCl-Co (31.67 kJ/mol). Although many studies have thoroughly investigated the $NaBH_4$ methanolysis with metal-free or metallic catalysts, investigations with propylene glycol/methanol mixtures are still limited. This research gap underlines the originality of the current study and shows the great potential of Ac-HCl-Fe as an effective catalyst for hydrogen generation.

Table 1. Comparison of HGRs and Ea of various catalyst systems in the $NaBH_4$ solvolysis reaction.

Catalysts	Solvent	Temp. (°C)	HGR ($mLmin^{-1}g_{cat}^{-1}$)	Ea (kJ/mol)	Ref.
ZnPc	Methanol	30	8993	28.47	[19]
MF	Methanol	30	20540	16,98	[20]
GW-HCl-Ni-Cat	Methanol	30	6643	18.68	[29]
MPÇ-HCl-kat	Methanol	30	10823	14.08	[32]
MPÇ-HCl-Ni-kat	Methanol	30	13125	20.43	[32]
Chit/Mont/H	Propylene glycol/methanol	30	40396	27.53	[45]
Banana peel	Methanol	30	65625	4.56	[47]
SSMS-$ZnCl_2$-CoB	Methanol	30	9266	31.13	[48]
P-doped g-C_3N_4	Methanol	30	8666	30.30	[49]
N,P-doped Chit@kaolin	Methanol/glycerol	30	36231	17.20	[50]
DS-HCl-Co	Methanol	30	8299	31.67	[51]
Co@AC	Water	30	8593	31.19	[52]
Co@CHE	Water	30	32036	55.6	[53]
Co@VHE	Water	25	36624	55	[54]
Ru@CQDs	Water	30	167588	38.19	[55]
Ac-HCl-Fe	Methanol	30	8486	---	This study
Ac-HCl-Fe	Propylene glycol/methanol	30	67820	32.36	This study

Catalyst reusability is an important factor in assessing its practical applicability. The reusability of Ac-HCl-Fe for hydrogen generation was evaluated over four consecutive cycles under the same conditions, as presented in Fig. 6a. Each test was conducted at 30 °C using 25 mg of Ac-HCl-Fe to catalyze the reaction of 0.25 g $NaBH_4$ in 10 mL of propylene glycol/methanol mixture. After each cycle, the catalyst was fully recovered, washed with distilled water, and dried in an oven at 100 °C. Although complete conversion was achieved in each cycle, a gradual decline in catalytic activity was observed. The HGR value of Ac-HCl-Fe was 67820 $mLmin^{-1}g_{cat}^{-1}$ during its first use, decreasing to 58564 $mLmin^{-1}g_{cat}^{-1}$ after the second cycle. By the final cycle, the HGR had further declined to 36782 $mLmin^{-1}g_{cat}^{-1}$, with the catalyst retaining only 54.2% of its initial activity (Fig. 6b).

To evaluate the catalyst's performance, the activity percentage was calculated by comparing the initial hydrogen yield with the yields obtained in subsequent $NaBH_4$ solvolysis cycles over a five-second interval. The results for Ac-HCl-Fe are shown in Fig. 6b. The data show a gradual decrease in catalytic activity, dropping from an initial 100% to 86.4%, 65.3%, and finally 54.2% over four consecutive cycles. The pronounced decrease in activity is likely attributable to the loss of Ac-HCl-Fe during the washing steps or the degradation of active sites within the catalyst structure [56]. Another possible explanation for this observation is the accumulation of $NaB(OCH_3)_4$ in the solution, formed from $NaBH_4$ degradation during solvolysis, along with the increased solution viscosity—both of which may contribute to the decrease in catalytic performance [57]. Accordingly, the decrease in catalytic efficiency over multiple cycles emphasizes the need for further studies to improve the catalyst regeneration method in order to maintain the activity of Ac-HCl-Fe in repeated applications.

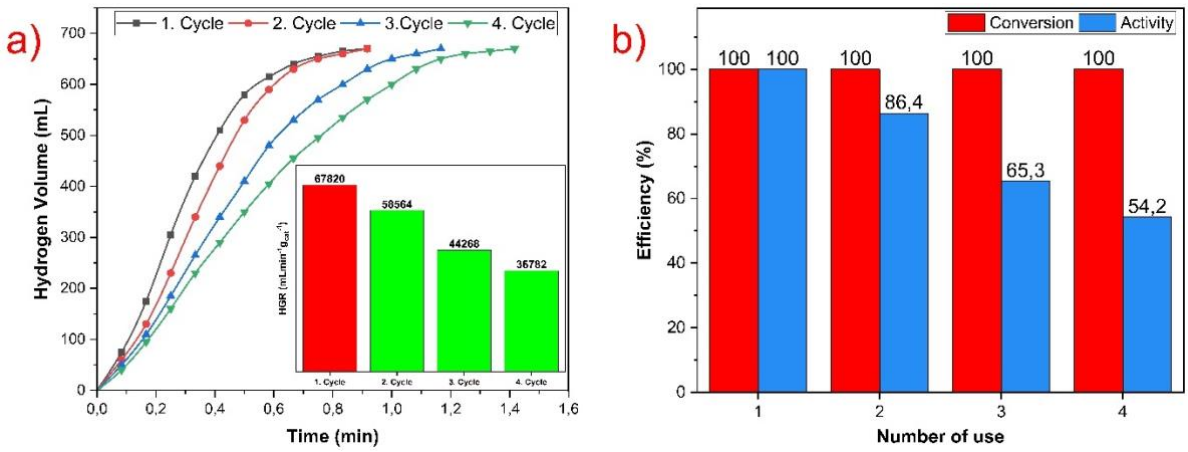

Fig. 6. (a) Effect of reusability on H_2 production from $NaBH_4$ in a 10 mL propylene glycol/methanol mixture using an Ac-HCl-Fe catalyst; (b) Profile of catalytic activity [Reaction condition: 25 mg catalyst, 0.25 g $NaBH_4$, 10 mL propylene glycol/methanol (1:1, v/v), 30 °C].

To investigate the reason behind the observed decrease in catalytic activity, the elemental composition of the Re-Ac-HCl-Fe catalyst was analyzed after four consecutive reaction cycles. This investigation included both SEM images and SEM-EDX analyses (Fig. 7). When the SEM images of the Ac-HCl-Fe and Re-Ac-HCl-Fe catalysts were examined, both catalysts exhibited a similar, compact, and well-organized morphology. SEM-EDX analysis were performed on Re-Ac-HCl-Fe catalyst. The Ac-HCl-Fe catalyst elemental composition was found to be 53.34% C, 16.48% O, 0.16% Mg, 0.37% Ca, 23.36% Fe, and 6.29% Cl, whereas the Re-Ac-HCl-Fe catalyst contained 58.75% C, 17.37% O, 0.26% Mg, 0.59% Ca, 18.11% Fe, 1.53% Cl and 3.39% B. As shown in Fig. 7, the EDX data of the Re-Ac-HCl-Fe catalyst revealed a notable accumulation of boron and oxygen on the catalyst surface, which is believed to have played a significant role in the decline of catalytic activity. Furthermore, as shown in Fig. 7 (A4), the intensity of the peaks corresponding to the iron component decreased after four cycles of use, likely due to the washing process. Additionally, the dissolution of catalytic components in the alkaline environment of sodium borohydride may contribute to this effect. To mitigate these issues, optimizing the washing procedure and adjusting the pH of the reaction mixture to minimize the dissolution of catalytic components can enhance catalyst stability.

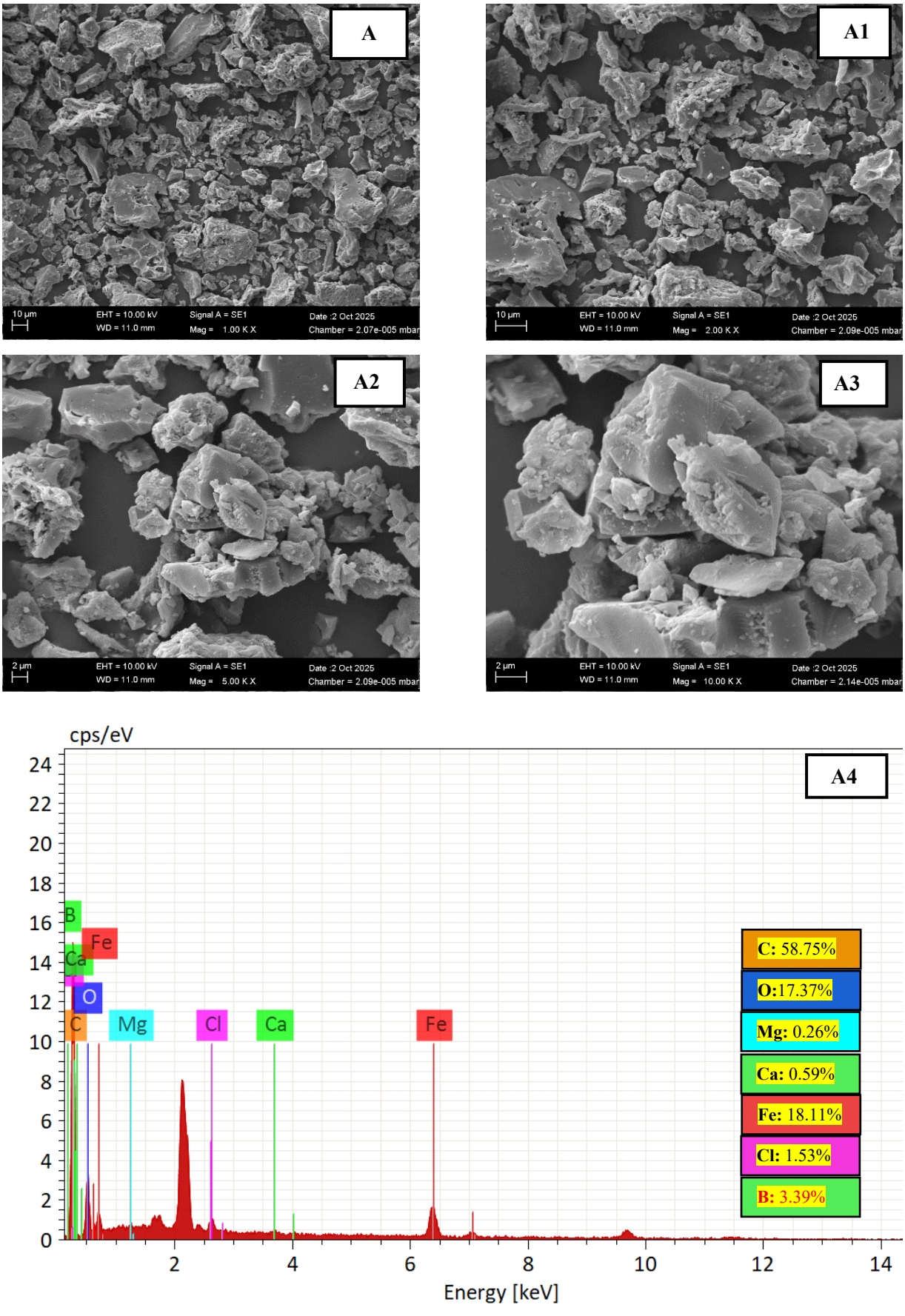

Fig. 7. SEM and SEM-EDX micrographs of the recycled catalyst (Re-Ac-HCl-Fe**)** (A–A4).

4. Conclusion

In this study, a novel activated carbon-based catalyst (Ac-HCl-Fe) was synthesized from acorn cup biomass through HCl-$FeCl_2$ co-activation, and its catalytic performance for hydrogen generation via the $NaBH_4$ solvolysis was evaluated for the first time. Comprehensive characterization of the Ac-HCl-Fe catalyst was carried out using FT-IR, SEM, and SEM-EDX analyses. To the best of our knowledge, this is one of the small number of studies to report on the use of a metal-supported activated carbon catalyst (Ac-HCl-Fe), derived from acorn cups waste for hydrogen production from $NaBH_4$ in a propylene glycol/methanol binary solvent system. The Ac-HCl-Fe catalyst exhibited outstanding catalytic performance, achieving an HGR of 67820 $mLmin^{-1}g_{cat}^{-1}$ at 30 °C—surpassing the hydrogen generation rates of previously reported active carbon-based catalysts. The apparent activation energy for the solvolysis reaction catalyzed by Ac-HCl-Fe was calculated to be 32.36 kJ/mol, further confirming its high efficiency. Reusability tests show that, despite the very short reaction times, the catalytic activity of Ac-HCl-Fe decreased by approximately 50% after the fourth cycle. Therefore, future studies may focus on improving its stability over multiple uses and evaluating its performance under more practical and scalable operating conditions. In addition, in future studies, the effects of different solvent types and ratios (Water/PG/MeOH) on reaction kinetics and catalytic performance will be systematically investigated.

Ethical statement

Not applicable.

Acknowledgments

The authors are thankful to Artvin Coruh University Scientific Research Project Coordination for supporting this research (Project Number: 2023.TAB.F65.02.01).

Conflict of Interest

The authors declare no conflicts of interest.

Authors' Contributions

U. I: Conceptualization; investigation; methodology; data curation; visualization; formal analysis; resources; writing—original draft; writing—review and editing.

Generative AI statement

The author(s) declare that no Gen AI was used in the creation of this manuscript.

References

[1] Chamoun, R., Demirci, U. B., and Miele, P., "Cyclic dehydrogenation–(re) hydrogenation with hydrogen-storage materials: An overview," *Energy Technology*, *3*(2), 100-117, 2015. https://doi.org/10.1002/ente.201402136

[2] Rusman, N. A. A., & Dahari, M., "A review on the current progress of metal hydrides material for solid-state hydrogen storage applications," *International Journal of Hydrogen Energy*, *41*(28), 12108-12126, 2016. https://doi.org/10.1016/j.ijhydene.2016.05.244

[3] Veziroğlu, T. N., & Şahi, S., "21st Century's energy: Hydrogen energy system," *Energy conversion and management, 49(7),* 1820-1831, 2008. https://doi.org/10.1016/j.enconman.2007.08.015

[4] Veziroglu, T. N., "Conversion to hydrogen economy," *Energy Procedia*, *29*, 654-656, 2012.

[5] Sahaym, U., & Norton, M. G. , "Advances in the application of nanotechnology in enabling a 'hydrogen economy'," *Journal of Materials Science*, *43*(16), 5395-5429, 2008. https://doi.org/10.1007/s10853-008-2749-0

[6] Durbin, D. J., & Malardier-Jugroot, C., "Review of hydrogen storage techniques for on board vehicle applications," *International journal of hydrogen energy*, *38*(34), 14595-14617, 2013. https://doi.org/10.1016/j.ijhydene.2013.07.058

[7] Midilli, A., Ay, M., Dincer, I., & Rosen, M. A., "On hydrogen and hydrogen energy strategies: I: current status and needs," *Renewable and sustainable energy reviews*, *9*(3), 255-271, 2005. https://doi.org/10.1016/j.rser.2004.05.003

[8] Ibrahim, A., Paskevicius, M., & Buckley, C. E., "Chemical compression and transport of hydrogen using sodium borohydride," *Sustainable Energy & Fuels*, *7*(5), 1196-1203, 2023. https://doi.org/10.1039/D2SE01334G

[9] Council, H., "Hydrogen for net zero-A critical cost-competitive energy vector," 2021. https://hydrogencouncil.com/en/hydrogen-for-net-zero/

[10] Jorgensen, S. W., "Hydrogen storage tanks for vehicles: Recent progress and current status," *Current Opinion in Solid State and Materials Science*, *15*(2), 39-43, 2011. https://doi.org/10.1016/j.cossms.2010.09.004

[11] Kılınç, D., Şahin, Ö., & Saka, C., "Salicylaldimine-Ni complex supported on Al2O3: Highly efficient catalyst for hydrogen production from hydrolysis of sodium borohydride," *International Journal of Hydrogen Energy*, *43*(1), 251-261, 2018. https://doi.org/10.1016/j.ijhydene.2017.10.151

[12] Saka, C., Yıldız, D., Kaya, S., Caglar, A., Elitok, D., Yaylı, E., ... & Kivrak, H., "A novel hazelnutt bagasse based activated carbon as sodium borohydride methanolysis and electrooxidation catalyst," *International Journal of Hydrogen Energy*, *48*(65), 25339-25353, 2023. https://doi.org/10.1016/j.ijhydene.2023.03.261

[13] Saka, C., "Phosphorus and oxygen doped carbon-based on Spirulina microalgae as efficient metal-free catalysts to obtain H2 from methanolysis of NaBH4," *International Journal of Hydrogen Energy*, *46*(5), 3753-3762, 2021. https://doi.org/10.1016/j.ijhydene.2020.08.222

[14] Sahiner, N., & Demirci, S., "Natural microgranular cellulose as alternative catalyst to metal nanoparticles for H2 production from NaBH4 methanolysis," *Applied Catalysis B: Environmental*, *202*, 199-206, 2017. https://doi.org/10.1016/j.apcatb.2016.09.028

[15] Sahiner, N., Yasar, A. O., & Aktas, N., "H2 generation from NaBH4 methanolysis via magnetic field sensitive ionic liquid coated silica particles as catalyst," *Surfaces and Interfaces*, *8*, 36-44, 2017. https://doi.org/10.1016/j.surfin.2017.04.006

[16] Ould-Amara, H., Alligier, D., Petit, E., Yot, P. G., & Demirci, U. B., "Sodium borohydride and propylene glycol, an effective combination for the generation of 2.3 wt% of hydrogen," *International Journal of Hydrogen Energy*, *43*(15), 7237-7244, 2018. https://doi.org/10.1016/j.ijhydene.2018.02.169

[17] Demirci, U. B., Akdim, O., Andrieux, J., Hannauer, J., Chamoun, R., & Miele, P., "Sodium borohydride hydrolysis as hydrogen generator: issues, state of the art and applicability upstream from a fuel cell," *Fuel Cells*, *10*(3), 335-350, 2010. https://doi.org/10.1002/fuce.200800171

[18] F Abdulaziz, F., El-Tantawy, A. I., Humaidi, J. R., Aljaloud, A. S., Azhary, A., Alanazi, A. A., ... & Taha, T. A. M., "Structure-performance relationship of SrTiO3/S@ g-C3N4 nanocomposites for highly active hydrogen production via NaBH4 methanolysis," *Diamond and Related Materials*, *148*, 111389, 2024. https://doi.org/10.1016/j.diamond.2024.111389

[19] Işik, U., Namli, M., Kantar, C., & Karakaş, D. E., "Zinc phthalocyanine as a heterogeneous catalyst for efficient H2 generation from NaBH4 methanolysis," *International Journal of Hydrogen Energy*, *176*, 151497, 2025. https://doi.org/10.1016/j.ijhydene.2025.151497

[20] Isik, U., Gultekin, E., Karakas, D. E., & Kaya, M., "Synthesis and characterization of triazole-based schiff bases as novel highly efficient organocatalysts for rapid H2 generation via NaBH4 methanolysis," *Fuel*, *406*, 137052, 2026. https://doi.org/10.1016/j.fuel.2025.137052

[21] Karakaş, D. E., "A novel cost-effective catalyst from orange peel waste protonated with phosphoric acid for hydrogen generation from methanolysis of NaBH4," *International Journal of Hydrogen Energy*, *47*(24), 12231-12239, 2022. https://doi.org/10.1016/j.ijhydene.2021.09.102

[22] Schlesinger, H. I., Brown, H. C., Finholt, A. E., Gilbreath, J. R., Hoekstra, H. R., & Hyde, E. K., "Sodium borohydride, its hydrolysis and its use as a reducing agent and in the generation of hydrogen1," *Journal of the American Chemical Society*, *75*(1), 215-219, 1953. https://doi.org/10.1021/ja01097a057

[23] Xu, D., Dai, P., Guo, Q., & Yue, X., "Improved hydrogen generation from alkaline NaBH4 solution using cobalt catalysts supported on modified activated carbon," *International journal of hydrogen energy*, *33*(24), 7371-7377, 2008. https://doi.org/10.1016/j.ijhydene.2008.09.065

[24] Wang, Y., Liu, J., Wang, K., Chen, T., Tan, X., & Li, C. M., "Hydrogen storage in Ni–B nanoalloy-doped 2D graphene," *International Journal of Hydrogen Energy*, *36*(20), 12950-12954, 2011. https://doi.org/10.1016/j.ijhydene.2011.07.034

[25] Barghi, S. H., Tsotsis, T. T., & Sahimi, M., "Chemisorption, physisorption and hysteresis during hydrogen storage in carbon nanotubes," *International journal of hydrogen energy*, *39*(3), 1390-1397, 2014. https://doi.org/10.1016/j.ijhydene.2013.10.163

[26] Long, J. J., Wu, H. C., Liu, Y. T., Ding, Y. Y., Yao, Q. L., Metin, O., & Lu, Z. H., "Hydrogen production from chemical hydrogen storage materials over copper-based catalysts," *CMat*, *1*(1), e10, 2024. https://doi.org/10.1002/cmt2.10

[27] Yang, Y. W., Lu, Z. H., & Chen, X. S., "Cu-based nanocatalysts for hydrogen generation via hydrolysis and methanolysis of ammonia borane," *Materials Technology*, *30*(sup2), A89-A93, 2015. https://doi.org/10.1179/17535557A15Y.000000004

[28] Han, Y., Ma, J., Wang, X., Wang, Y., Zhang, K., Cao, Z., ... & Li, G., "Preparation of Co–P–B/foam Ni catalyst and its catalytic performance for hydrogen production by hydrolysis of NaBH4 solution," *Fuel*, *372*, 132262, 2024. https://doi.org/10.1016/j.fuel.2024.132262

[29] Karakaş, D. E., Horoz, S., Durap, F., Orak, C., & Kaya, M., "Integrated catalytic and energy storage performance of grass waste derived ni-based catalyst," *Arabian Journal for Science and Engineering*, *50*(6), 4209-4221, 2025. https://doi.org/10.1007/s13369-024-09564-8

[30] Lam, E., & Luong, J. H., "Carbon materials as catalyst supports and catalysts in the transformation of biomass to fuels and chemicals," *ACS catalysis*, *4*(10), 3393-3410, 2014. https://doi.org/10.1021/cs5008393

[31] Lin, T., Chen, I. W., Liu, F., Yang, C., Bi, H., Xu, F., & Huang, F., "Nitrogen-doped mesoporous carbon of extraordinary capacitance for electrochemical energy storage," *Science*, *350*(6267), 1508-1513, 2015. https://doi.org/10.1126/science.aab3798

[32] E. M. Kalkan, " Synthesis of oak acorn cup-supported metal-doped/metal-free catalysts and investigation of catalytic activities in sodium borohydride methanolysis reactions," Master's Thesis, Siirt University, Siirt, Türkiye, 2023.

[33] Asmae, B., Ahmed, B., Benaouda, B., Saleh, Y. S. G., Benderdouche, N., Ali, Ç., ... & Michalkiewicz, B., "Selected pharmaceutical pollutant recovery from wastewater by an agro-byproduct Laurus nobilis-based adsorbent: Theoretical and experimental studies," *Journal of the Taiwan Institute of Chemical Engineers*, *170*, 106011, 2025. https://doi.org/10.1016/j.jtice.2025.106011

[34] Zhang, Y., Zhang, C., Li, W., Xiao, Q., Jiao, F., Xu, S., ... & Cao, W., "Reaction mechanism of stearic acid pyrolysis via reactive molecular dynamics simulation and TG-IR technology," *Renewable Energy*, *217*, 119115, 2023. https://doi.org/10.1016/j.renene.2023.119115

[35] Feng, J., Zhu, H., Xu, Y., Jiang, J., & Pan, H., "Preparation and characterization of high-performance activated carbon from papermaking black-liquor at low temperature," *Journal of Analytical and Applied Pyrolysis*, *159*, 105292, 2021. https://doi.org/10.1016/j.jaap.2021.105292

[36] Aziz, E. K., Abdelmajid, R., Rachid, L. M., & Mohammadine, E. H., "Adsorptive removal of anionic dye from aqueous solutions using powdered and calcined vegetables wastes as low-cost adsorbent," *rab Journal of Basic and Applied Sciences*, *25*(3), 93-102, 2018. https://doi.org/10.1080/25765299.2018.1517861

[37] Tetsuka, H., Nagoya, A., Fukusumi, T., & Matsui, T., "Molecularly Designed, Nitrogen-Functionalized Graphene Quantum Dots for Optoelectronic Devices," *Advanced Materials (Deerfield Beach, Fla.)*, *28*(23), 4632-4638, 2016. https://doi.org/10.1002/adma.201600058

[38] Masanizan, A., Lim, C. M., Kooh, M. R. R., Mahadi, A. H., & Thotagamuge, R., "The removal of ruthenium-based complexes N3 dye from DSSC wastewater using copper impregnated KOH-activated bamboo charcoal," *Water, Air, & Soil Pollution*, *232*(9), 388, 2021. https://doi.org/10.1007/s11270-021-05333-7

[39] Das, P., Sreelatha, T., & Ganesh, A., "Bio oil from pyrolysis of cashew nut shell-characterisation and related properties," *Biomass and bioenergy*, *27*(3), 265-275, 2004. https://doi.org/10.1016/j.biombioe.2003.12.001

[40] Rahayu, N. W. S. T., Park, J., Yang, M., Wang, S., & Lee, M., "Cesium removal from a water system using a polysulfone carrier containing nitric acid-treated bamboo charcoal," *Journal of Environmental Radioactivity*, *225*, 106374, 2020. https://doi.org/10.1016/j.jenvrad.2020.106374

[41] Xu, N., Gao, S., Xu, C., Fang, Y., Xu, L., & Zhang, W., "Carbon quantum dots derived from waste acorn cups and its application as an ultraviolet absorbent for polyvinyl alcohol film," *Applied Surface Science*, *556*, 149774, 2021. https://doi.org/10.1016/j.apsusc.2021.149774

[42] Xu, D., Lai, X., Guo, W., Zhang, X., Wang, C., & Dai, P., "Efficient catalytic properties of SO42−/MxOy (M= Cu, Co, Fe) catalysts for hydrogen generation by methanolysis of sodium borohydride," *International Journal of Hydrogen Energy*, *43*(13), 6594-6602, 2018. https://doi.org/10.1016/j.ijhydene.2018.02.074

[43] Sahiner, N., & Demirci, S., "Very fast H2 production from the methanolysis of NaBH4 by metal-free poly (ethylene imine) microgel catalysts," *International Journal of Energy Research*, *41*(5), 736-746, 2017. https://doi.org/10.1002/er.3679

[44] Bekirogullari, M., "Hydrogen production from sodium borohydride by ZnCl2 treated defatted spent coffee ground catalyst," *International journal of hydrogen energy*, *45*(16), 9733-9743, 2020. https://doi.org/10.1016/j.ijhydene.2020.01.244

[45] Saka, C., "Fabrication of protonated chitosan/montmorillonite catalyst for hydrogen production via sodium borohydride in the optimum methanol/propylene glycol mixture," *International Journal of Hydrogen Energy*, *65*, 410-420, 2024. https://doi.org/10.1016/j.ijhydene.2024.03.371

[46] Khan, M. S. J., Alkhadher, S. A. A., Sidek, L. M., Kamal, T., Asiri, A. M., Khan, S. B., ... & Ahmed, A. N., "Metal nanoparticles entrapment in chitosan-carbon black composite hydrogel towards sustainable environmental solutions," *International Journal of Biological Macromolecules*, *296*, 139717, 2025. https://doi.org/10.1016/j.ijbiomac.2025.139717

[47] Elma Karakaş, D., Kaya, M., & Horoz, S., "Efficient hydrogen generation from the NaBH4 methanolysis by waste material: banana peel," *Carbon Letters*, *32*(6), 1593-1601, 2022. https://doi.org/10.1007/s42823-022-00391-1

[48] Kaya, M., Bekiroğullari, M., & Saka, C., "Highly efficient CoB catalyst using a support material based on Spirulina microalgal strain treated with ZnCl2 for hydrogen generation via sodium borohydride methanolysis," *International journal of energy research*, *43*(9), 4243-4252, 2019. https://doi.org/10.1002/er.4548

[49] Saka, C., "Facile fabrication of P-doped g-C3N4 particles with nitrogen vacancies for efficient dehydrogenation of sodium borohydride methanolysis," *Fuel*, *313*, 122688, 2022. https://doi.org/10.1016/j.fuel.2021.122688

[50] Saka, C., "Use of two-component methanol/glycerol solvent system as an alternative to single-component solvent systems in hydrogen production with sodium borohydride and design of phosphorus, nitrogen co-doped chitosan/kaolin composite with heterojunction as metal-free catalyst," *International Journal of Hydrogen Energy*, *98*, 1007-1019, 2025. https://doi.org/10.1016/j.ijhydene.2024.12.134

[51] Karakaş, D. E., Kaya, M., , & Horoz, S., "Catalytic activites of a biomaterial (sumac) catalyst in sodium borohyride methanolysis reactions," *Journal of Molecular Structure*, *1273*, 134276, 2023. https://doi.org/10.1016/j.molstruc.2022.134276

[52] Ekinci, S., & Onat, E. "Activated carbon assisted cobalt catalyst for hydrogen production: synthesis and characterization." *Balıkesir Üniversitesi Fen Bilimleri Enstitüsü Dergisi*, *26*(2), 455-471, 2024. https://doi.org/10.25092/baunfbed.1297146

[53] Onat, E., Ekinci, S., Izgi, M. S., Erkan, E., Atiç, S., Kocaman, B., & Tümen, V. "Sustainable hydrogen production from NaBH4 using Co@CHE Catalyst: Experimental and MLP-Based modeling for autonomous fuel systems." *Fuel*, *406*, 136999, 2026. https://doi.org/10.1016/j.fuel.2025.136999

[54] Onat, E., Alan, Y., Savcı, A., Ekinci, S., & İzgi, M. S. "Green-synthesized Co@VHE nanocatalyst from Verbascum insulare for enhanced hydrogen generation and biological applications." *Biomass and Bioenergy*, *204*, 108435, 2026. https://doi.org/10.1016/j.biombioe.2025.108435

[55] Onat, E., İzgi, M. S., Şahin, Ö., & Ekinci, S. "Enhanced Hydrogen Production from Sucrose-Derived Carbon Quantum Dots-Supported Ru Catalysts: A Comparative Study of KBH4 and NaBH4 Hydrolysis." *Renewable Energy*, 123692, 2025. https://doi.org/10.1016/j.renene.2025.123692

[56] Gokkus, K., Ozbal, A., Senturan, U. M., Gür, M., & Bütün, V., "Synthesis of azo polymers and their catalytic performance in hydrogen production via NaBH4 methanolysis," *Materials Research Bulletin*, *180*, 113009, 2024. https://doi.org/10.1016/j.materresbull.2024.113009

[57] Gao, Z., Ding, C., Wang, J., Ding, G., Xue, Y., Zhang, Y., ... & Gao, X., "Cobalt nanoparticles packaged into nitrogen-doped porous carbon derived from metal-organic framework nanocrystals for hydrogen production by hydrolysis of sodium borohydride," *International Journal of Hydrogen Energy*, *44*(16), 8365-8375, 2019. https://doi.org/10.1016/j.ijhydene.2019.02.008